OXFORD

SOT | Society of Toxicology
www.toxsci.oxfordjournals.org

TOXICOLOGICAL SCIENCES, 146(2), 2015, 354–362

doi: 10.1093/toxsci/kfv101
Advance Access Publication Date: May 20, 2015
Research Article

Interactive Effects of N6AMT1 and As3MT in Arsenic Biomethylation

Hao Zhang,[*,1] Yichen Ge,[*,1,2] Ping He,[†] Xushen Chen[*], Abreu Carina,[*] Yulan Qiu,[*] Diana S. Aga,[†] and Xuefeng Ren,[*,‡,3]

[*]Department of Epidemiology and Environmental Health; [†]Department of Chemistry; and [‡]Department of Pharmacology and Toxicology, The State University of New York, Buffalo, New York

[1]These authors contributed equally to this study.
[2]Present address: Guangdong Provincial Key Laboratory of Occupational Disease Prevention and Treatment, Guangdong Prevention and Treatment Center for Occupational Diseases, Guangzhou 510300, People's Republic of China.
[3]To whom correspondence should be addressed at 276 Farber Hall, University at Buffalo, Buffalo, NY 14221. Fax: (716) 829-2979. E-mail: xuefengr@buffalo.edu.

ABSTRACT

In humans, arsenic is primarily metabolized by arsenic (+3 oxidation state) methyltransferase (As3MT) to yield both trivalent and pentavalent methylated metabolites. We recently reported that the putative N-6 adenine-specific DNA methyltransferase 1 (N6AMT1) can biotransform monomethylarsonous acid (MMA^{III}) to dimethylarsinic acid, conferring resistance of human cells to arsenic exposure. To further decipher the role of N6AMT1 and its interaction with As3MT in arsenic biomethylation, we examined the relative contribution of N6AMT1 and As3MT in metabolizing arsenic using several newly modified UROtsa human urothelial cells, ie, UROtsa cells with either a constant level of N6AMT1 or As3MT in combination with an inducible level of As3MT or N6AMT1, respectively. Our analysis confirmed the involvement of N6AMT1 in MMA^{III} biomethylation but not for inorganic arsenic. In a comparable level of N6AMT1 and As3MT, the effect of N6AMT1 mediated MMA^{III} biomethylation was obscured by the action of As3MT. Furthermore, we showed that the levels of N6AMT1 and As3MT proteins varied among and within human normal and cancerous tissues. Overall, the data showed that N6AMT1 has a role in MMA^{III} biomethylation, but its effect is relatively minor and limited compared with As3MT. In addition, the varied levels and distributions of N6AMT1 and As3MT among human tissues may potentially contribute to the tissue specificity and susceptibility to arsenic toxicity and carcinogenicity.

Key words: arsenic metabolism; As3MT; N6AMT1

Consumption of drinking water contaminated with inorganic arsenic (iAs), a natural and carcinogenic metalloid, constitutes a major public health problem (Abernathy *et al.*, 1999; Tapio and Grosche, 2006). Human epidemiological studies have shown that chronic arsenic exposure via drinking water is associated with increased morbidity and mortality from both cancerous and noncancerous effects, such as skin and internal cancers, diabetes, peripheral neuropathy, and cardiovascular diseases (Chen *et al.*, 1988; Chen and Ahsan, 2004; Mumford *et al.*, 2007; Smith *et al.*, 1998, 2006; Tseng *et al.*, 1968).

Although the precise modes of action for many adverse effects of arsenic remain under intense investigations, it is well accepted that arsenic metabolism in humans and other mammals plays a central role in its toxic and carcinogenic activity (Drobna *et al.*, 2005; Ferrario *et al.*, 2008; Kligerman *et al.*, 2003; Li *et al.*, 2005; Thomas *et al.*, 2007; Wei *et al.*, 2002). The discovery of arsenic (+3 oxidation state) methyltransferase (As3MT) enzyme has been a major breakthrough in understanding the relationship between arsenic biomethylation and the modes of action of arsenic (Thomas *et al.*, 2007). In humans, arsenic is converted to trivalent and pentavalent mono- and dimethylated metabolites, primarily by As3MT, with dimethylarsinic acid (DMA^{V}) being the major metabolite excreted from urine. Although there remain different opinions, the conversion of iAs to DMA^{V} is

considered a detoxification mechanism because the toxicity of DMA^V is lower than that of iAs (Styblo *et al.*, 2000). However, arsenic methylation can also be a bioactivation process because the toxicity of intermediate metabolites such as monomethylarsonous acid (MMA^{III}) is much higher than that of iAs in terms of acute toxicity (Styblo *et al.*, 2000). Human epidemiology studies have suggested that variability in arsenic biomethylation and the resulting changes of arsenic metabolite profiles, in particular the elevated ratio between mono- and dimethylated metabolites in urine and blood, is associated with an increased susceptibility to skin lesions (Valenzuela *et al.*, 2009) and several types of cancer (Ahsan *et al.*, 2007; Chung *et al.*, 2010; De Chaudhuri *et al.*, 2008; Lin *et al.*, 2006).

We recently reported that N-6 adenine-specific DNA methyltransferase 1 (N6AMT1), a putative methyltransferase, was one of the promising methyltransferases involved in arsenic methylation (Ren *et al.*, 2011). We demonstrated that in contrast to As3MT, which methylates iAs to the mono- and dimethylated arsenicals, N6AMT1 appears to be specifically involved in the conversion of MMA^{III} to the less toxic DMA^V. A follow-up study examining the relationship of *N6AMT1* polymorphism in arsenic methylation efficiency in humans showed a positive association that is independent of *As3MT* (Harari *et al.*, 2013). Altogether, these studies suggest that N6AMT1 may be a new arsenic metabolizing methyltransferase, and its genetic variation could affect the arsenic metabolism and subsequent susceptibility to arsenic-associated adverse effects. However, it is clear that the research related to N6AMT1 is still in the early stage and more studies are needed to gain a better understanding of its role in arsenic metabolism and toxicity.

The aim of this study was to investigate the interactive effects of N6AMT1 and As3MT in modulating arsenic metabolism and cytotoxicity. To this end, we modified human urothelial cells, the UROtsa cell, and established several cell lines with either a constant level of N6AMT1 or As3MT protein, and at the same time with an inducible level of As3MT or N6AMT1 protein. These model cells enabled us to examine the relative contribution of N6AMT1 and As3MT in metabolizing arsenic.

MATERIALS AND METHODS

Chemicals and Reagents

Sodium arsenite ($NaAsO_2$ '[iAs^{III}]; purity > 99%) was purchased from Sigma-Aldrich (St Louis, Missouri). Diiodomethylarsine (MMA^{III}) was a generous gift from Dr A. Jay Gandolfi (University of Arizona, Tucson, Arizona). iAs^{III} and MMA^{III} solutions were freshly prepared using sterile water (MilliQ; Millipore, Billerica, Massachusetts) and protected from light before use. Doxycycline (Dox) was purchased from SigmaAldrich (St Louis). Dulbecco's modified eagle medium (DMEM) was acquired from Life Tech (Carlsbad, California). Fetal bovine serum (FBS) was obtained from Lonza Group Ltd (Walkersville, Maryland); Penicillin-Streptomycin and 1 × trypsin-Ethylenediaminetetraacetic acid (EDTA) (0.25%) were from Cellgro Mediatech Inc (Manassas, Virginia). Anti-β-actin and anti-N6AMT1 antibodies were obtained from Sigma-Aldrich (St Louis). Anti-As3MT was purchased from Santa Cruz Bio (Dallas, Texas). Peroxidase-conjugated Anti-Rabbit IgG antibody was from Jackson Immuno Research (West Grove, Pennsylvania). Recombinant human N6AMT1 and As3MT proteins were received from Life Tech and Abnova (Walnut, California), respectively.

Cell Lines and Arsenic Treatment

The UROtsa cells, which is an immortalized cell line derived from a primary culture of normal human uroepithelium, were chosen as our study model for arsenic methylated metabolism due to its relatively low level of N6AMT1 protein and no detectable level of As3MT protein. UROtsa cells were generously shared by Dr Zuzana Drobna (University of North Carolina, Chapel Hill). Human embryonic kidney cell HEK293 was purchased from ATCC (Manassas, Virginia) and RetroPack PT67 and Lenti-X 293T cells were purchased from Clontech (Mountain View, California). The cell lines were maintained in DMEM supplemented with 10% FBS and penicillin-streptomycin and incubated at 37°C in a fully humidified atmosphere containing 5% CO_2. UROtsa cells were treated with iAs^{III} at concentrations from 0 to 50 μM or MMA^{III} at 0–5 μM when 70%–80% confluency was reached in culture.

N6AMT1 and As3MT Gene Expression Vector Constructs and Stabilized Cells

Human *N6AMT1* (GenBank accession No.NM_013240) or As3MT (GenBank accession No.NM_020682.3) cDNAs were amplified using primers 5′- AACGCAGCGAAGGACTAT-3′ & 5′- CAGTAGT TCTGGGCACAC-3′, and 5′-GGAGACATGGCTGCACTTCGT-3′ & 5′-GATCACTCTTGCCCACTACTG-3′, respectively. The PCR products were gel purified (Qiagen, Valencia, California) and cloned into pCR2.1-TOPO vector (Invitrogen) according to the manufacturer's instructions, and the sequence was confirmed. For *N6AMT1* gene, the pCR2.1-TOPO vector containing the N6AMT1 gene was excised using NotI/BamHI restriction enzymes (New England Biolabs, Ipswich, Massachusetts) and subjected to gel purification. The nucleotides of the N6AMT1 gene containing BamHI and NotI overhangs were annealed and ligated to a linearized pRetro X-IRES-ZsGreen vector (Clontech) digested with BamHI and NotI (New England Biolabs). For constructing the pLVX-TRE3G-mCherry containing N6AMT1 gene, human *N6AMT1* gene was amplified using primers 5′- GAGACGC GTAACGCAGCGAAGGACTATGGC-3′ and 5′- GTCCATATGCAG TAGTTCTGGGCACACACT-3′. PCR product and pLVX-TRE3G-mCherry vector were excised using MluI/NdeI restriction enzymes (New England Biolabs) and then ligated to generate the pLVX-TRE3G-mCherry vector containing *N6AMT1* gene. For *As3MT* gene, the pCR2.1-TOPO vector containing the *As3MT* gene was excised and *As3MT* gene was cloned into pRetroX-IRES-ZsGreen1 and pLVX-TRE3G-mCherry vectors following the similar strategy as cloning N6AMT1 gene. Retrovirus and lentivirus containing either *N6AMT1* or *As3MT* gene were produced according to the manufacturer's protocols (Clontech) in RetroPack PT67 and Lenti-X 293T cells, respectively. The viral supernatant was collected and stored in aliquots at −80°C for later use.

To generate UROtsa cells with the stabilized expression of *N6AMT1* or *As3MT* gene, UROtsa cells were infected with the constructed retrovirus or an empty vector counterpart. The viral supernatant was diluted to half with culture medium, and polybrene added at a concentration of 8 μg/ml. The cell culture medium was exchanged with viral supernatant. At 24 h after infection, the viral supernatant was replaced with fresh medium. After 48–72 h, cells were assessed by an AMG EVOS XL microscope (Advanced Microscopy Group, Bothell, Washington). The ZsGreen fluorescent marker yields a bright green fluorescence, permitting direct monitoring of the delivery efficiency. Finally, the cell populations were sorted by the Becton Dickenson FACSAria II high speed 10-color cell sorter (BD, Franklin Lakes, New Jersey), and cells with green fluorescent

were purified and collected. The collected cells were named as URO-R, URO-R/As3, and URO-R/N6, respectively.

To generate UROtsa cells with constant level of N6AMT1 or As3MT in combination with inducible levels of As3MT or N6AMT1, the earlier generated cells, URO-R, URO-R/As3, and URO-R/N6, were further infected by the collected lentivirus. Following similar steps as mentionedearlier, we generated UROtsa cells with a constant level of N6AMT1 but an inducible level of As3MT, named as URO-R/N6-L-As3. Similarly, we named UROtsa cells with a constant level of As3MT and an inducible level of N6AMT1 as URO-R/As3-L/N6. The control containing both control retrovirus and lentivirus was named as URO-R-L.

Image Analysis of Established Cells

To examine the expression of *N6AMT1* and *As3MT*, in particular the inducible effect, the established cells were treated with Dox at concentrations of 0, 10, 100 ng/ml. After 24 h culture, the cells were monitored using Zeiss Axio Observer Fluorescence Microscopy Systems and photographs were taken using Zeiss AxioVision software (Zeiss, Pleasanton, California) (Fig. 1).

Quantification of N6AMT1 and As3MT Protein Levels

After 24 h Dox induction, total cell lysates were prepared from 5×10^6 cells using 300 µl of radioimmunoprecipitation assay lysis buffer. Total protein was quantified using Bio-Rad DC assay reagent (Bio-Rad). An equal amount of total protein (30 µg) from all samples was separated by SDS-PAGE and electrotransferred onto nitrocellulose membrane. In addition, known amounts of purified N6AMT1 or As3MT proteins, from 0.625 to 10 ng, were also loaded on the gel to serve as standards for quantification. Anti-As3MT, anti-N6AMT1, and anti-β-actin antibodies were immunoblotted. Proteins were visualized using the WesternBright ECL western blotting detection kit (Advansta Inc Menlo Park, California). Films were then exposed and developed using the Konica SRX-101 developer (Wayne, New Jersey). β-Actin was used as loading control.

Arsenic Species Profile Analysis by High-Performance Liquid Chromatography/Inductively Coupled Plasma–Mass Spectrometry

Established cells were cultured in DMEM medium and treated by various concentration of iAs^{III} or MMA^{III} for 24 h. Culture media were collected and stored at −80°C until analysis. Samples were diluted 1:5 with mobile phase only before immediate use. Analysis of the various speciation of arsenic was performed using a high-performance liquid chromatography system (Thermo HPLC Spectra System) coupled to an inductively coupled plasma mass spectrometer (Thermo X-Series 2 ICP-MS). Separation was achieved using an ion-pair chromatography column (Gemini-NX-C18 column, 3 µm × 4.6 mm id × 150 mm) equipped with a guard column (Gemin-NX C18, 4 × 3.0 mm id, Phenomenex Inc). Instrument conditions were modified based on a previously published method (Kalman *et al.*, 2014). The optimized conditions for ICP-MS and HPLC settings are given in Table 1. The detailed reagents preparation and related data can be found in the supplementary information. HPLC was run using Thermo Xcalibur software and the ICP-MS data were collected and processed using Thermo PlasmaLab software.

MTT Analysis

The 3-(4,5-dimethyl thiazol-2-yl)-2,5-diphenyl-2H-tetrazolium bromide (MTT) assay was performed to assess cell viability after

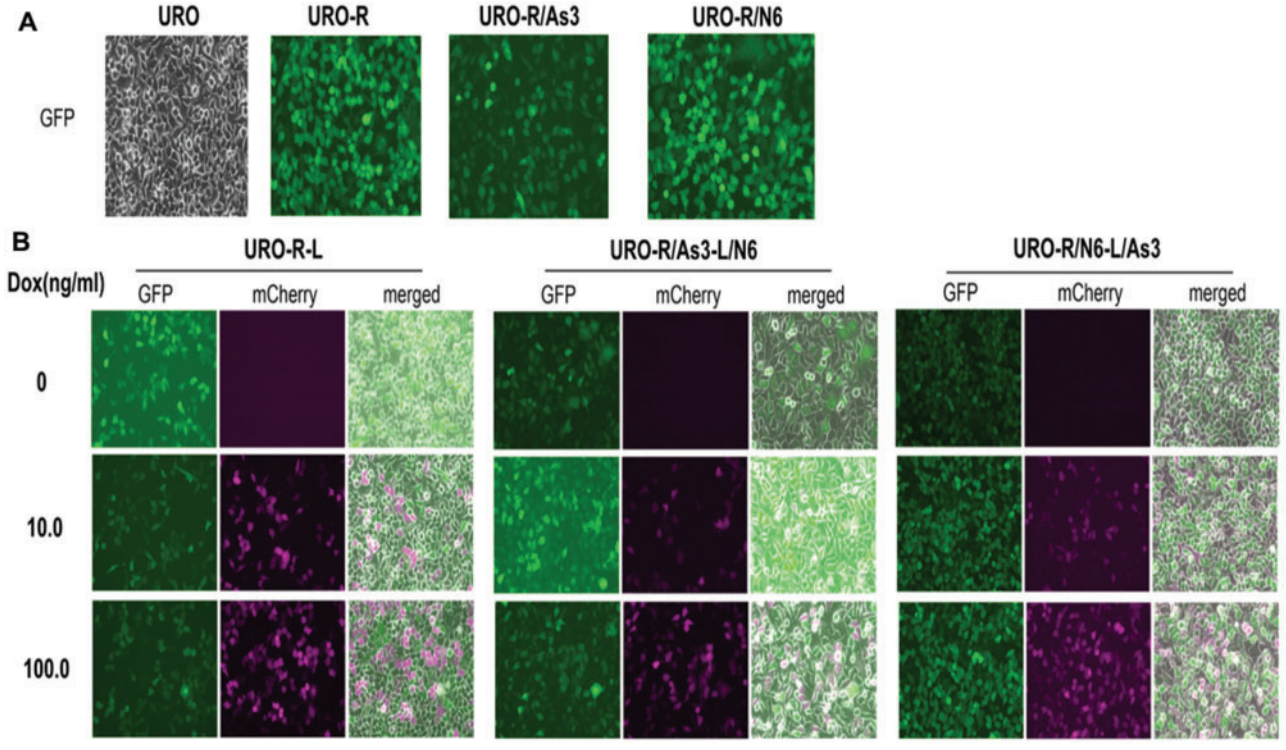

FIG. 1. Establish stabilized UROtsa cell lines with a constant level of N-6 adenine-specific DNA methyltransferase 1 (N6AMT1) or arsenic (+3 oxidation state) methyltransferase (As3MT) in combination with an inducible level of As3MT or N6AMT1. A, Representative images of UROtsa cells infected with either retrovirus control or retrovirus containing N6AMT1 or As3MT, showing the cell lines were positive with the expression of ZsGreen fluorescent marker; B, Representative images of established UROtsa cell lines post 24 h Dox treatment. Administration of Dox induced a dose-dependent increase of the m-cherry fluorescence, indicating a workable induction cell model.

TABLE 1. Instrument Conditions Used for Arsenic Speciation

ICP-MS conditions[a]	RF power	1350 W
	Nebulizer gas flow	0.8 l/min
	Auxiliary gas flow	0.8 l/min
	Plasma gas flow	15 l/min
	nebulizer	concentric
HPLC conditions	Column	Gemini-NX-C18 column from Phenomenex, 3 μm × 4.6 mm id × 150 mm, 110 Å
	Mobile phase	20 mM $(NH_4)_2CO_3$ containing 5 mM tetrabutylammonium hydroxide and 2.5% methanol
	Flow rate	1 ml/min
	Injected Volume	100 μl

[a]May slightly change based on daily performance.

arsenic treatment. Cells were cultured in 96-well plates in a volume of 100 μl medium/well at a density of 5×10^4 cells/ml. Twenty four hours after incubation with iAs^{III} or MMA^{III} (6 replicates/arsenical concentration), 10 μl sterile MTT dye (Sigma-Aldrich; 5 mg/ml) was added to each well, and plates were incubated at 37°C for 4 h. The culture medium was then removed, and 200-μl dimethyl sulfoxide was added and thoroughly mixed for 10 min. Absorbance measurements were performed at 570 nm using a 96-well microplate reader.

Immunohistochemistry and Data Analysis

TMA and patient population. N6AMT1 protein expression was assessed using the tissue microarray (TMA) and comprised 23 tumor tissue types and nonmatching normal tissue control collected from patients diagnosed at Roswell Park Cancer Institute (RPCI) between 1993 and 2009. Three 0.6-mm tissue cores of formalin-fixed paraffin-embedded tissue were arrayed into recipient paraffin blocks. To identify representative tumor areas, an experienced pathologist evaluated H&E-stained slides of all blocks prior to construction of the TMA.

Immunohistochemistry, slide scanning, and image analysis. The Immunohistochemistry (IHC) staining for N6AMT1 was optimized by the Pathology Resource Facility at Roswell Park Cancer Institute. The detailed methods can be found in the supplementary information. TMA slides were digitally scanned using Aperio ScanScope (Aperio Technologies, Inc, Vista, California) with 20× bright-field microscopy. These images were then accessible using Spectrum (Aperio Technologies, Inc), a web-based digital pathology information management system. Slide images were automatically associated to a digital slide created in the Digital Slide table in Spectrum. Once slides were scanned, Aperio ImageScope version 11.2.0.780 (Aperio Technologies, Inc) was used to view images for image analysis. A unique algorithm was created for N6AMT1 stained tissue. Positivity thresholds were set for the positive stain, and the scores for average cytoplasmic intensity for the selected regions were calculated based on these thresholds. Cells were individually classified as 0-none, 1+-weak, 2+ -moderate, and 3+ -Strong. The algorithm used color deconvolution that separates the hematoxylin and 3,3′-Diaminobenzidine (DAB) stains, thereby providing stain separation. The analysis results provided the total number of detected cells, the percentage of cells per class (0, 1+, 2+, and 3+), and the percentage of positive stained cells along with the average staining intensity of the positive cells as a score of 0, 1+, 2+, and 3+. Additionally the H-score was calculated. The H-score is an intensity score derived from the average intensity of the staining of the cytoplasm according to the threshold intervals set in the algorithm macro. This score = 1*(%1+) + 2*(%2+) + 3*(%3+) when the score is between 0 and 300, where 300 represents 100% of cells being 3+.

Analysis of N6AMT1 and As3MT IHC Data Obtained from Protein Atlas Organization

After we finished our IHC analysis of N6AMT1 protein, Human Protein Atlas also released the IHC data of N6AMT1 that was not available before. We thus also downloaded the IHC data of N6AMT1 and As3MT protein from online database of Human Protein Atlas (http://www.proteinatlas.org/) (Mosca *et al.*, 2013; Ponten *et al.*, 2008). It included the data of N6AMT1 and As3MT protein level in different normal human tissues and cancer types, which were classified as none (N), weak (W), moderate (M), and strong (S) based on protein levels. We calculated the percentage of staining intensity in each classification (Supplementary Table S3).

Statistical Analysis

The reported values represent the means ± SDs for at least 3 independent experiments performed in triplicate. One-way Analysis of variance (ANOVA) was used to compare the difference among groups. Jonckheere's 2-sided trend test was performed with respect to the cell death estimates as a function of increasing MMA^{III} concentration between the cell lines. Data were analyzed using SAS 9.2 unless otherwise mentioned (SAS Institute Inc Cary, North Carolina).

RESULTS

Quantification of N6AMT1 or As3MT Protein Levels in the Established UROtsa Cell Lines

Figure 2 showed the results of western blot analysis of As3MT and N6AMT1protein levels in the established UROtsa cell lines. Compared with control URO-R cells that have no detectable level of As3MT, As3MT protein was increased in URO-R/As3 cells but not in URO-R/N6 cells. Similarly, the level of N6AMT1 protein was increased in URO-R/N6 cells but not in URO-R/As3 cells. For URO-R/As3-L/N6 and URO-R/N6-L/As3 cells, a gradually increased level of As3MT or N6AMT1was observed post the administration of Dox. However, we do observe a base level of As3MT and N6AMT1 protein in these cells, indicating that the culture medium may contain trace level of Dox-like chemicals even though cells were cultured in commercial Dox-free cell culture medium. Similar results were observed in the mRNA level of As3MT or N6AMT1 in these cells by semiquantitative reverse transcription-PCR (RT-PCR) (data not shown). Utilizing the recombinant human N6AMT1 and As3MT proteins as standard, we calculated the protein levels in the established cells (Supplementary Table S1). The level of As3MT and N6AMT1 proteins in URO-R/As and URO-R/N6 cells is 5.89 ± 2.44 ng per million cells and 8.75 ± 1.54 ng per million cells, respectively. At Dox 10 and 100 μg/ml levels, the levels of As3MT or N6AMT1 proteins cells were 8.89 ± 2.65 and 11.71 ± 3.24 ng per million cells in URO-R/N6-L/As3 and 7.31 ± 1.98 and 11.90 ± 3.02 in URO-R/As3-L/N6.

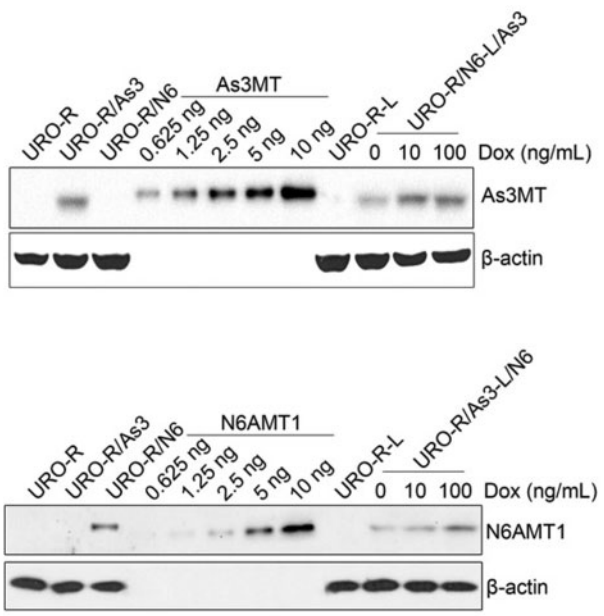

FIG. 2. Quantification of N6AMT1 and As3MT protein levels in established UROtsa cell lines. Western blot analysis shows increased levels of N6AMT1 and As3MT proteins in URO-R/N6 and URO-R/As3 cells, respectively. A gradually increased level of N6AMT1 or As3MT was observed post the administration of Dox in URO-R/As3-L/N6 and URO-R/N6-L/As3 cells.

Arsenic Metabolism by N6AMT1 and As3MT

The HPLC-ICP-MS was used to determine methylation states of arsenicals in cultures of these modified UROtsa cells ie, URO-R, URO-R/As3, URO-R/N6, URO-R-L, URO-R/As3-L/N6, and URO-R/N6-L/As3 cells. Our pilot analyses showed that the levels of arsenicals in cell extracts are significantly lower (< 3%) than that in culture medium. Therefore, here we reported only the results of arsenic metabolites analysis in culture medium.

There were no detectable levels of methylated arsenicals in either cell lysates or culture medium of URO-R, URO-R/N6, URO-R-L, and URO-R/N6-L/As3 (no Dox treatment) cells after exposure to iAs^{III} for 24 h. In comparison, methylated arsenicals including MMA^{III}, MMA^{V}, and DMA^{V} were detected both in the cell lysates and cell culture medium of URO-R/As3, URO-R/As3-L/N6, and URO-R/N6-L/As3 cells (with Dox treatment) (data not shown).

Table 2 and Supplementary Table S2 provide the arsenic speciation results of cells exposure to MMA^{III} for 24 h. Control URO-R and URO-R-L cells have no arsenic methylation capacity. As a result, no detectable levels of iAs and dimethylated arsenicals were observed in these 2 cell types (Supplementary Table S2). In URO-R/N6 cells, approximately 1%–2% of MMA^{III} initially added into the culture were converted to DMA^{V} over the 24 h culture periods (Table 2). The methylation rates were significantly increased in the URO-R/N6-L/As3 cells when they were pretreated with Dox for 24 h. The percentage of DMA^{V} versus $MMA^{(III+V)}$ in the culture medium was up to 26.1% with 10 ng/ml Dox treatment and 79.6% with 100 ng/ml Dox treatment (Table 2). In URO-R/As3 cells, the percentage of DMA^{V} versus $MMA^{(III+V)}$ was in the range from 27.1% to 4.7%, and it was decreased proportionally with the increased MMA^{III} concentration. Unexpectedly, the conversion of MMA^{III} to DMA^{V} is much higher in the URO-R/As3-L/N6 cells than in the URO-R/As cells even before the Dox treatment. The percentage of DMA^{V} versus $MMA^{(III+V)}$ is 54.1% in URO-R/As3-L/N6 cells compared with 27.1% in URO-R/As3 cells with 0.1μM MMA^{III} exposure. Pretreatment with Dox in URO-R/As3-L/N6 cells apparently didn't change the arsenic methylation significantly, although the percentage of DMA^{V} versus $MMA^{(III+V)}$ appeared to increase, especially in the lower doses of MMA^{III} treatment (Table 2).

Increased Levels of N6AMT1 and As3MT Protein and MMA^{III}-Induced Cytotoxicity

Figure 3 showed that MMA^{III} treatments induced a dose-dependent decrease in the viability of all cell lines. Jonckheere's 2-sided trend test was performed with respect to the cell death estimates as a function of increasing MMA^{III} concentration between cells with increased levels of N6AMT1 and/or As3MT proteins and control URO-R or URO-R-L cells. No significant differences were observed in the comparison between any cell lines, suggesting that there is no difference in the overall sensitivity to MMA^{III} exposure (P value > .05, data not shown).

The increased levels of N6AMT1 protein did not have any significant effect in the cytotoxicity of MMA^{III} in each administered dose level when compared URO-R/N6 cells with the control URO-R cells (Fig. 3B). In comparison, the increased As3MT protein levels were associated with a significantly increased resistance to MMA^{III} exposure at both 1 and 3μM levels in URO-R/As3 cells relative to the control URO-R cells (Fig. 3C). Similarly, without Dox treatment, there were no observed differences of cytotoxicity between URO-R/N6-L/As3 cells and URO-R-L cells, and the differences were found at 1 and 3μM MMA^{III} levels between URO-R/As3-L/N6 cells and URO-R-L cells. With the pretreatment of Dox at 10 or 100 μg/ml, there was an increased resistance to MMA^{III}-induced cytotoxicity at 1 μM level in the URO-R/N6-L/As3 cells (Fig. 3E), but no effects in the URO-R/As3-L/N6 cells (Fig. 3F).

Differential Levels of N6AMT1 and As3MT Proteins in Human Normal and Cancer Tissues

Table 3 contains results of N6AMT1 and As3MT protein levels in selected human tissues that are considered as potential cancerous targets for arsenicals. The complete data containing all human normal and cancer tissues are shown in Supplementary Table S3. The data reported here is for the entire tissue and a result mainly from the evaluation of the protein levels in epithelial cells in the tissues. Our analysis using TMA set from RPCI showed that N6AMT1 protein levels were classified as weak in the human liver, lung, and stomach tissues and moderate in the kidney tissue. However, N6AMT1 protein levels were rated from moderate to strong in these same normal tissues using the data obtained from Human Protein Atlas. The level of As3MT protein was classified strong in the stomach tissue, moderate in the bladder, liver, and lung tissue, and weak in the kidney and skin. In general, the level of N6AMT1 protein in cancer tissues was comparable to the level in normal tissues, but the As3MT protein level was lower in cancer tissues than in the normal tissues (Table 3).

DISCUSSION

In this study of the interactive effects of N6AMT1 and As3MT in arsenic metabolism, our data suggested that the effects of N6AMT1 in arsenic metabolism are relatively minor and limited when compared with the action of As3MT.

It has long been hypothesized that there may exist additional arsenic-metabolizing methyltransferases besides the As3MT. Studies showed that loss of As3MT expression in human cells (Drobna *et al.*, 2006) and in mice (Drobna *et al.*, 2009)

TABLE 2. MMA^{III} Metabolism in Cells of URO-R/As, URO-R/As-L/N6, URO-R/N6, and URO-R/N6-L/As

Cells	Dox (ng/ml)	$MMA^{(III+V)}$			DMA^{V}			DMA^{V} versus $MMA^{(III+V)}$		
		(Mean [ppb] + STD)			[Mean (ppb) + STD]			(%+STD)		
		0	10	100	0	10	100	0	10	100
URO-R/N6	[MMA^{III}]μM									
	0	ND	N/A	N/A	ND	N/A	N/A	N/A	N/A	N/A
	0.1	23.0 + 4.8	N/A	N/A	0.5 + 0.5	N/A	N/A	1.8 + 1.7	N/A	N/A
	0.3	63.4 + 12.4	N/A	N/A	0.5 + 0.5	N/A	N/A	0.9 + 1.0	N/A	N/A
	0.5	96.5 + 10.5	N/A	N/A	1.8 + 0.5	N/A	N/A	1.8 + 0.3	N/A	N/A
	1.0	291.3 + 46.8	N/A	N/A	4.0 + 2.7	N/A	N/A	1.3 + 0.7	N/A	N/A
	3.0	554.3 + 44.5	N/A	N/A	1.5 + 0.7	N/A	N/A	0.2 + 0.1	N/A	N/A
URO-R/N6-L/As3	[MMA^{III}]μM									
	0	ND	ND	ND	ND	ND	ND	N/A	N/A	N/A
	0.1	11.6 + 2.5	6.9 + 1.2	13.8 + 3.7	0.5 + 0.3	1.7 + 0.4	2.7 + 0.4	4.2 + 2.0	26.1 + 11.4	19.8 + 3.3
	0.3	51.6 + 4.8	29.9 + 3.9	23.9 + 5.9	1.5 + 0.3	6.4 + 1.4	8.5 + 0.4	2.9 + 0.8	22.2 + 7.7	36.9 + 7.9
	0.5	86.9 + 10.4	70.5 + 9.5	23.9 + 11.1	1.4 + 0.4	9.1 + 0.9	16.8 + 2.3	1.6 + 0.6	12.9 + 0.7	79.6 + 31.0
	1.0	184.00 + 23.3	141.3 + 26.3	56.4 + 17.4	1.9 + 0.3	11.1 + 2.1	21.3 + 5.7	1.1 + 0.3	7.8 + 1.3	38.1 + 1.8
	3.0	459.4 + 27.4	430.9 + 8.6	286.1 + 28.8	1.8 + 0.8	7.8 + 0.9	49.3 + 20.9	0.4 + 0.2	1.8 + 0.7	16.9 + 5.6
URO-R/As3	[MMA^{III}]μM									
	0	ND	N/A	N/A	ND	N/A	N/A	N/A	N/A	N/A
	0.1	15.4 + 1.4	N/A	N/A	4.1 + 2.4	N/A	N/A	27.1 + 16.1	N/A	N/A
	0.3	79.8 + 17.8	N/A	N/A	15.5 + 3.6	N/A	N/A	19.3 + 1.1	N/A	N/A
	0.5	117.7 + 10.6	N/A	N/A	16.0 + 0.9	N/A	N/A	13.6 + 0.4	N/A	N/A
	1.0	262.7 + 32.2	N/A	N/A	24.0 + 7.2	N/A	N/A	9.5 + 3.9	N/A	N/A
	3.0	451.8 + 11.4	N/A	N/A	21.2 + 11.0	N/A	N/A	4.7 + 2.3	N/A	N/A
URO-R/As3-L/N6	[MMA^{III}]μM									
	0	ND	ND	ND	ND	ND	ND	N/A	N/A	N/A
	0.1	9.9 + 0.8	11.10 + 1.0	15.2 + 0.8	5.3 + 0.8	2.4 + 0.6	3.6 + 1.0	54.1 + 12.0	21.2 + 4.5	23.1 + 5.5
	0.3	31.9 + 4.8	15.7 + 0.9	18.8 + 0.6	13.2 + 0.5	9.2 + 0.7	11.3 + 1.0	42.2 + 7.8	58.8 + 7.6	60.2 + 3.5
	0.5	38.9 + 6.3	28.4 + 2.5	27.9 + 0.8	19.4 + 1.2	15.9 + 1.4	16.4 + 1.1	51.1 + 11.3	55.6 + 4.1	58.9 + 2.2
	1.0	75.1 + 13.2	68.2 + 6.1	94.0 + 3.2	31.3 + 4.0	25.5 + 1.7	35.9 + 2.1	41.9 + 2.1	37.2 + 1.4	38.2 + 3.6
	3.0	379.6 + 46.0	380.2 + 31.9	475.6 + 28.6	26.0 + 1.4	30.4 + 4.4	20.4 + 3.2	7.0 + 1.2	8.1 + 1.9	4.3 + 0.4

does not completely eliminate the capacity to methylate arsenic. We recently showed that N6AMT1 may be another methyltransferase involved in human arsenic metabolism, specifically converting high toxic MMA^{III} to the less toxic DMA^{V} (Ren *et al.*, 2011). This observation was once again confirmed in this study (Table 2). However, the metabolizing rate mediated by N6AMT1 is lower when compared with the previous study. The percentage of di- versus monomethylated arsenicals ranged from 1.8% to 0.3% in culture medium of URO-R/N6 cells in comparison to the range from 20% to 5% in the previous study. The exact reason is unknown for the observed differences in the N6AMT1 mediated reaction, but it could be due to the different levels of N6AMT1 protein in the cells examined.

To more precisely compare the biomethylation efficiency between As3MT and N6AMT1, we quantified the protein levels of N6AMT1 and As3MT in the established URO-R/N6 and URO-R/As3 cells (Fig. 2 and Supplementary Table S1). The levels of N6AMT1 and As3MT proteins were largely comparable between URO-R/N6 and URO-R/As3 cells. However, the rate in converting MMA^{III} to DMA^{V} was significantly different between these 2 cell lines. Treatment with MMA^{III} resulted in an increased level of DMA^{V} in the media after 24 h both in URO-R/N6 and URO-R/As3 cells. However, the level of DMA^{V} in URO-R/N6 was much lower in comparison to URO-R/As3 cells, and the percentage of DMA^{V} versus $MMA^{(III+V)}$ level in the culture medium ranged from 1.8% to 0.3%, and from 27.1% to 4.7% in the URO-R/N6 and URO-R/As3 cells, respectively. Additionally, with the presence of As3MT protein in the cells (URO-R/As-L/N6), Dox-induced increase of N6AMT1 protein level did not significantly alter the MMA^{III} biomethylation profiles even though the levels of N6AMT1 protein were almost 2-fold higher than the As3MT protein levels (Table 2 and Supplementary Table S1). In comparison, the increase of As3MT protein level in N6AMT1 expressed URO-R/N6-L/As3 cells led to an increased percentage of DMA^{V} versus $MMA^{(III+V)}$ (Table 2). Furthermore, the increased level of N6AMT1 protein did not significantly change the viability after MMA^{III} treatment at all concentrations tested compared with the control cells, although the URO-R/N6 cells seem more resistant at 1μM MMA^{III} level (the viability changed from 69% to 77%). The increased resistance to MMA^{III} treatment was observed in cells with an increased level of As3MT protein, eg, in the URO-R/As3, URO-R/As-L/N6, and the Dox-treated URO-R/N6-L/As3 cells. Altogether, the data suggest that the enzymatic activities of As3MT-mediated MMA^{III} biomethylation are much higher than the reaction mediated by N6AMT1 protein.

Previously we showed that the mRNA level of *N6AMT1* was relatively low in most measured tissues compared with the mRNA level of *As3MT* (Ren *et al.*, 2011). This time we were able to compare the protein levels of N6AMT1 and As3MT. Using the data obtained from Human Protein Atlas, the levels of N6AMT1 protein were relatively stable and classified as moderate in most of the human normal tissues examined (Table 3 and Supplementary Table S3). In comparison between Human Protein Atlas and our own IHC data, N6AMT1 protein levels were comparable in 3 tissues (Kidney, Ovary, and Prostate), and were different in 4 other tissues (Liver, Lung, Spleen, Stomach), in which N6AMT1 protein levels were classified as weak in our IHC data, but classified as moderate, strong, moderate, and

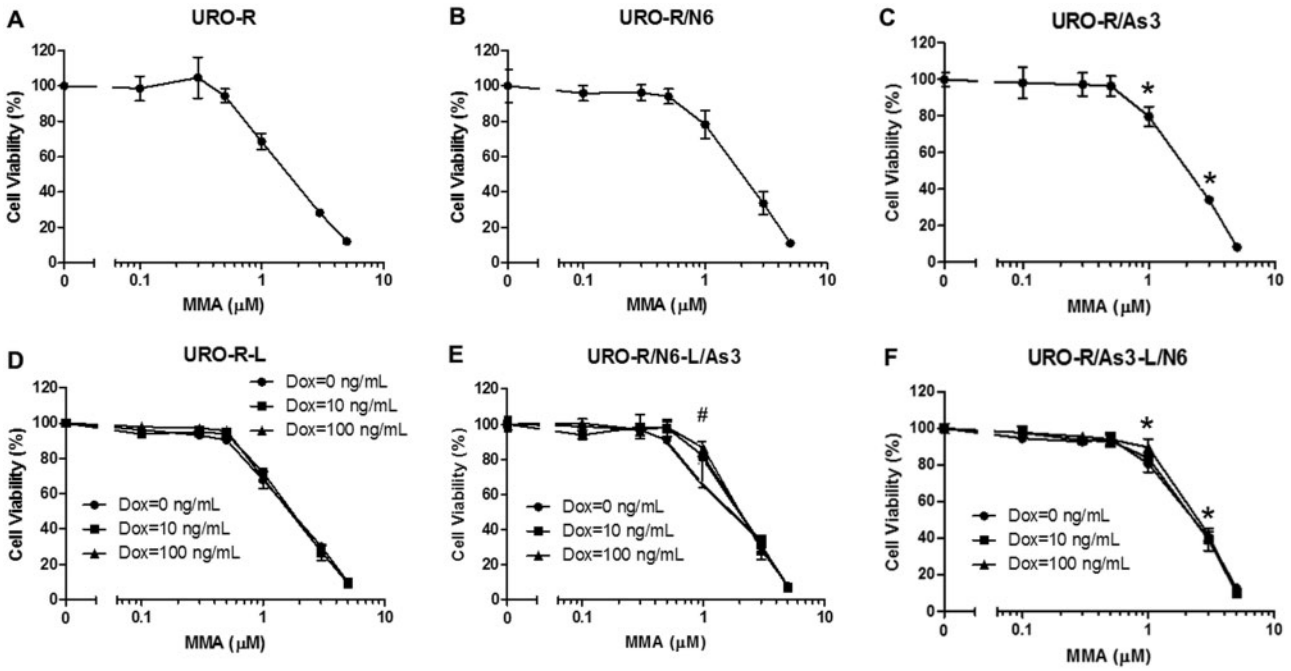

FIG. 3. Elevated levels of human N6AMT1 and/or As3MT protein have no overall impact on monomethylarsonous acid (MMA^{III})-induced cytotoxicity. A dose-dependent decrease in viability of all cell lines was observed after MMA^{III} exposure (A, URO-R; B, URO-R/N6; C, URO-R/As3; D, URO-R-L; E, URO-R/N6-L/As3, and F, URO-R/As3-L/N6). Jonckheere's 2-sided trend test was performed and showed that there were no significant differences of MMA^{III}-induced cytotoxicity in the comparison between any cell lines (P value $> .05$). Elevated As3MT protein levels in UROtsa cells led to resistance to MMA^{III} at 1 and 3μM levels (D and F; *P value $< .05$). Dox induced increase of As3MT protein level could alter the susceptibility of UROtsa cells to MMA^{III} exposure when N6AMT1 protein presented (E; #P value $< .05$).

TABLE 3. N6AMT1 and As3MT Protein Levels in Selected Human Normal and Cancer Tissues

Tissue		N6AMT1				N6AMT1[f]				As3MT[f]			
		Staining Intensity (%)				Staining Intensity (%)				Staining Intensity (%)			
		S[a]	M[b]	W[c]	N[d]	S	M	W	N	S	M	W	N
Bladder	Normal						Y[e]				Y		
	Tumor		40	60			82	18				45	55
Kidney	Normal		Y				Y					Y	
	Tumor		30	70			50	50			27	64	9
Liver	Normal			Y			Y				Y		
	Tumor		40	60			92	8			66	33	
Lung	Normal			Y		Y					Y		
	Tumor		12	35	53	18	73	9			16	42	42
Skin	Normal						Y					Y	
	Tumor		35	65		8	59	33			10	45	45
Stomach	Normal			Y			Y			Y			
	Tumor		40	60		8	75	17			46	27	27

[a]strong (S), [b]moderate (M), [c]weak (W), [d]none (N), and [e]Yes (Y); [f]Data are from Human Protein Atlas (http://www.proteinatlas.org/).

moderate in the Human Protein Atlas data, respectively. As3MT protein levels were varied among the human normal tissues; about half were classified as moderate and half were weak, and several tissues were rated as strong in the Human Protein Atlas data (Supplementary Table S3). It appeared that the levels and distributions of the N6AMT1 and As3MT protein are different among the normal tissues. For example, N6AMT1 protein levels were classified either as weak or moderate in the human liver tissues, but rated strong for the As3MT levels. In kidney and prostate, N6AMT1 protein levels are moderate in comparison to As3MT protein that was rated as weak. Another observation is that the level of N6AMT1 protein in most cancer tissues was comparable to the levels in normal tissues, but the As3MT protein level was lower in cancer tissues in comparison to normal tissues. A recent study showed that genetic polymorphisms of *N6AMT1* were significantly associated with the %MMA in urine (Harari *et al.*, 2013). It suggests that the altered function of N6AMT1 may have an impact on the arsenic metabolism and subsequent toxicity, indicating that the varied levels of N6AMT1 among tissues or the individuals may also have effects on arsenic toxicity. However, it is clear that this is just the first step in determining whether the different levels of N6AMT1 and As3MT proteins among the human tissues could contribute to the tissue specificity and human genetic susceptibility of

arsenic-induced toxicity and carcinogenicity. Additional studies in a more defined condition with a larger sample size are warranted to further clarify the association between arsenic tissue-specific metabolism and toxicity and the tissue distributions of N6AMT1 and As3MT proteins.

CONCLUSIONS

Using the newly established cell models with controlled levels of N6AMT1 and As3MT proteins, we confirmed our previous results indicating that N6AMT1 protein is involved in arsenic biomethylation, and specifically participating in the conversion of MMA^{III} to DMA^{V}. However, the role of N6AMT1 protein in arsenic metabolism is relatively minor and limited compared with the As3MT when their protein levels are comparable. The action of N6AMT1 in metabolizing MMA^{III} can be obscured by the action of As3MT, supporting the dominant and primary role of As3MT in arsenic metabolism. There remains need to determine if the observed differences in the levels and distributions of N6AMT1 and As3MT among human tissues could contribute to the tissue specificity and genetic susceptibility of arsenic-induced toxicity and carcinogenicity. We are in the process of determining the kinetic characters of N6AMT1 and As3MT in metabolizing MMA^{III}, which should help to further elucidate the role and the effects of N6AMT1 and As3MT on arsenic metabolism.

FUNDING

This work was supported by National Institutes of Health/National Institute of Environmental Health Sciences grants R21ES022329 and R01ES022629 to X.R.

SUPPLEMENTARY DATA

Supplementary data are available online at http://toxsci.oxfordjournals.org/.

REFERENCES

Abernathy, C. O., Liu, Y. P., Longfellow, D., Aposhian, H. V., Beck, B., Fowler, B., Goyer, R., Menzer, R., Rossman, T., Thompson, C.,*et al.* (1999). Arsenic: Health effects, mechanisms of actions, and research issues. *Environ. Health Perspect.* **107**, 593–597.

Ahsan, H., Chen, Y., Kibriya, M. G., Slavkovich, V., Parvez, F., Jasmine, F., Gamble, M. V., and Graziano, J. H. (2007). Arsenic metabolism, genetic susceptibility, and risk of premalignant skin lesions in Bangladesh. *Cancer Epidemiol. Biomarkers Prev.* **16**, 1270–1278.

Chen, Y., and Ahsan, H. (2004). Cancer burden from arsenic in drinking water in Bangladesh. *Am. J. Public Health* **94**, 741–744.

Chen, C. J., Kuo, T. L., and Wu, M. M. (1988). Arsenic and cancers. *Lancet* **1**, 414–415.

Chung, C. J., Pu, Y. S., Su, C. T., Chen, H. W., Huang, Y. K., Shiue, H. S., and Hsueh, Y. M. (2010). Polymorphisms in one-carbon metabolism pathway genes, urinary arsenic profile, and urothelial carcinoma. *Cancer Causes Control* **21**, 1605–1613.

De Chaudhuri, S., Ghosh, P., Sarma, N., Majumdar, P., Sau, T. J., Basu, S., Roychoudhury, S., Ray, K., and Giri, A. K. (2008). Genetic variants associated with arsenic susceptibility: Study of purine nucleoside phosphorylase, arsenic (+3) methyltransferase, and glutathione S-transferase omega genes. *Environ. Health Perspect.* **116**, 501–505.

Drobna, Z., Naranmandura, H., Kubachka, K. M., Edwards, B. C., Herbin-Davis, K., Styblo, M., Le, X. C., Creed, J. T., Maeda, N., Hughes, M. F., *et al.* (2009). Disruption of the arsenic (+3 oxidation state) methyltransferase gene in the mouse alters the phenotype for methylation of arsenic and affects distribution and retention of orally administered arsenate. *Chem. Res. Toxicol.* **22**, 1713–1720.

Drobna, Z., Waters, S. B., Devesa, V., Harmon, A. W., Thomas, D. J., and Styblo, M. (2005). Metabolism and toxicity of arsenic in human urothelial cells expressing rat arsenic (+3 oxidation state)-methyltransferase. *Toxicol. Appl. Pharmacol.* **207**, 147–159.

Drobna, Z., Xing, W., Thomas, D. J., and Styblo, M. (2006). shRNA silencing of AS3MT expression minimizes arsenic methylation capacity of HepG2 cells. *Chem. Res. Toxicol.* **19**, 894–898.

Ferrario, D., Croera, C., Brustio, R., Collotta, A., Bowe, G., Vahter, M., and Gribaldo, L. (2008). Toxicity of inorganic arsenic and its metabolites on haematopoietic progenitors "in vitro": Comparison between species and sexes. *Toxicology* **249**, 102–108.

Harari, F., Engstrom, K., Concha, G., Colque, G., Vahter, M., and Broberg, K. (2013). N-6-adenine-specific DNA methyltransferase 1 (N6AMT1) polymorphisms and arsenic methylation in Andean women. *Environ. Health Perspect.* **121**, 797–803.

Kalman, D. A., Dills, R. L., Steinmaus, C., Yunus, M., Khan, A. F., Prodhan, M. M., Yuan, Y., and Smith, A. H. (2014). Occurrence of trivalent monomethyl arsenic and other urinary arsenic species in a highly exposed juvenile population in Bangladesh. *J. Expos. Sci. Environ. Epidemiol.* **24**, 113–120.

Kligerman, A. D., Doerr, C. L., Tennant, A. H., Harrington-Brock, K., Allen, J. W., Winkfield, E., Poorman-Allen, P., Kundu, B., Funasaka, K., Roop, B. C.,*et al.* (2003). Methylated trivalent arsenicals as candidate ultimate genotoxic forms of arsenic: Induction of chromosomal mutations but not gene mutations. *Environ. Mol. Mutagen.* **42**, 192–205.

Li, J., Waters, S. B., Drobna, Z., Devesa, V., Styblo, M., and Thomas, D. J. (2005). Arsenic (+3 oxidation state) methyltransferase and the inorganic arsenic methylation phenotype. *Toxicol. Appl. Pharmacol.* **204**, 164–169.

Lin, G. F., Du, H., Chen, J. G., Lu, H. C., Guo, W. C., Meng, H., Zhang, T. B., Zhang, X. J., Lu, D. R., Golka, K.,*et al.* (2006). Arsenic-related skin lesions and glutathione S-transferase P1 A1578G (Ile105Val) polymorphism in two ethnic clans exposed to indoor combustion of high arsenic coal in one village. *Pharmacogenet. Genomics* **16**, 863–871.

Mosca, R., Pons, T., Ceol, A., Valencia, A., and Aloy, P. (2013). Towards a detailed atlas of protein-protein interactions. *Curr. Opin. Struct. Biol.* **23**, 929–940.

Mumford, J. L., Wu, K., Xia, Y., Kwok, R., Yang, Z., Foster, J., and Sanders, W. E. (2007). Chronic arsenic exposure and cardiac repolarization abnormalities with QT interval prolongation in a population-based study. *Environ. Health Perspect.* **115**, 690–694.

Ponten, F., Jirstrom, K., and Uhlen, M. (2008). The Human Protein Atlas–a tool for pathology. *J. Pathol.* **216**, 387–393.

Ren, X., Aleshin, M., Jo, W. J., Dills, R., Kalman, D. A., Vulpe, C. D., Smith, M. T., and Zhang, L. (2011). Involvement of N-6 adenine-specific DNA methyltransferase 1 (N6AMT1) in arsenic biomethylation and its role in arsenic-induced toxicity. *Environ. Health Perspect.* **119**, 771–777.

Smith, A. H., Goycolea, M., Haque, R., and Biggs, M. L. (1998). Marked increase in bladder and lung cancer mortality in a region of Northern Chile due to arsenic in drinking water. *Am. J. Epidemiol.* **147**, 660–669.

Smith, A. H., Marshall, G., Yuan, Y., Ferreccio, C., Liaw, J., von Ehrenstein, O., Steinmaus, C., Bates, M. N., and Selvin, S. (2006). Increased mortality from lung cancer and bronchiectasis in young adults after exposure to arsenic in utero and in early childhood. *Environ. Health Perspect.* **114**, 1293–1296.

Styblo, M., Del Razo, L. M., Vega, L., Germolec, D. R., LeCluyse, E. L., Hamilton, G. A., Reed, W., Wang, C., Cullen, W. R., and Thomas, D. J. (2000). Comparative toxicity of trivalent and pentavalent inorganic and methylated arsenicals in rat and human cells. *Arch. Toxicol.* **74**, 289–299.

Tapio, S., and Grosche, B. (2006). Arsenic in the aetiology of cancer. *Mutat. Res.* **612**, 215–246.

Thomas, D. J., Li, J., Waters, S. B., Xing, W., Adair, B. M., Drobna, Z., Devesa, V., and Styblo, M. (2007). Arsenic (+3 oxidation state) methyltransferase and the methylation of arsenicals. *Exp. Biol. Med.* **232**, 3–13.

Tseng, W. P., Chu, H. M., How, S. W., Fong, J. M., Lin, C. S., and Yeh, S. (1968). Prevalence of skin cancer in an endemic area of chronic arsenicism in Taiwan. *J. Natl. Cancer Inst.* **40**, 453–463.

Valenzuela, O. L., Drobna, Z., Hernandez-Castellanos, E., Sanchez-Pena, L. C., Garcia-Vargas, G. G., Borja-Aburto, V. H., Styblo, M., and Del Razo, L. M. (2009). Association of AS3MT polymorphisms and the risk of premalignant arsenic skin lesions. *Toxicol. Appl. Pharmacol.* **239**, 200–207.

Wei, M., Wanibuchi, H., Morimura, K., Iwai, S., Yoshida, K., Endo, G., Nakae, D., and Fukushima, S. (2002). Carcinogenicity of dimethylarsinic acid in male F344 rats and genetic alterations in induced urinary bladder tumors. *Carcinogenesis* **23**, 1387–1397.